Congress on Numerical Methods in Engineering 2011
Coimbra, 14 to 17 June, 2011

THE MOVING WINDOW METHOD AND TIME-DEPENDENT BOUNDARY CONDITIONS: APPLICATIONS TO HIGH-SPEED TRACKS

Z. Dimitrovová[1]* and A.F.S. Rodrigues[1]

1: UNIC, Department of Civil Engineering
Faculdade de Ciências e Tecnologia
Universidade Nova de Lisboa
Monte de Caparica, 2829-516 Caparica, Portugal
e-mail: zdim@fct.unl.pt, andre.rodrigues.fct@gmail.com

Keywords: Moving load, finite element method, quasi-stationary dynamic response, transient dynamic response, absorbing boundary conditions, plastic deformation

Abstract *Simplified models of railway tracks can provide quick reply to some fundamental issues. However, when nonlinear effects like irreversible ballast deformations are important, a detailed model involving all structural details is preferable. Such a model can be solved by the finite element method, but then it is difficult to choose the correct (i) size of the model, (ii) size of the finite elements and (iii) type of boundary conditions. Techniques based on a moving window method could overcome some of these difficulties. The moving window method is based on the assumption that the load is kept still, while the track model (or a part of it) moves in the direction opposing the originally supposed load movement. This can be accomplished by several techniques, from which the simplest one is to shift the results of the current time step against the load. Nevertheless, in commercial finite element software such an operation is usually protected against inappropriate usage. Alternatively, some results of the current time step can be moved in form of initial conditions for the next time step, but then, if the boundary conditions are violated, the results can start to diverge from the pretended objective.*

In this contribution two new techniques are proposed. The enhanced moving window method is introduced and implemented in commercial finite element software. In addition, and for handling irreversible nonlinearities, an approach based on time-dependent boundary conditions on the front and rear faces of the moving window is established. The methods proposed have several advantages, some of them are listed as: (i) the model itself can be rather small, but the time dependent results can cover an arbitrarily large model; (ii) quasi-stationary results can be obtained; (iii) in the linear case the effect of a set of loads can be achieved by superposition of previous results; (iv) in the nonlinear case the effect of repeated loads can be accounted for by implementation of the time-dependent boundary conditions. Several one- two- and three-dimensional case studies are analyzed. Influence of various parameters is studied. Accuracy is verified by comparison with analytical solutions or with results of the long simulation on large models. L^2-norm is used for accuracy evaluation.

1. INTRODUCTION

Railway transportation is facing the challenge of tailoring the railway system for the 21st century in order to improve its competiveness with airway transport. This increases demands on creating new lines, on modernization of existing lines and on increasing the capacity of the whole railway network. As a consequence, new issues related to the dynamic response of railway tracks to the moving load are still arising. It is necessary to have an efficient computational tool giving quick response with sufficient accuracy to the arising questions.

Simplified models of railway tracks are widely used because they can quickly provide a simple reply to some fundamental issues and have several other advantages [1, 2]. However, when nonlinear effects like irreversible ballast settlements are important, then a complete model involving all structural details is preferable. Such a model can be solved by the finite element method, but then it is difficult to choose the correct (i) size of the model, (ii) size of the finite elements and (iii) type of boundary conditions. The model itself must be large enough in order to eliminate satisfactorily transient effects due to a sudden placement of the load on the structure and, on the other hand, small enough to be computationally accessible. The edges of the finite elements must be sufficiently small in order to represent adequately propagating waves. The Rayleigh superficial waves have the lowest velocity of propagation, when compared with the shear and pressure waves. In soft soils it can be lower than 100m/s. The excitation frequency of the oscillating part of the moving load can be around 500-1000rad/s (for velocity 50-100m/s and sleepers spacing of 0.6m), which implies the wave lengths around 1-0.5m. Consequently, the elements on the subgrade surface should have the largest edge around 0.1-0.05m in soft soils. The boundary conditions are even more delicate issue. The dynamic analysis of solids of infinite dimensions with discrete methods such as finite elements calls for the use of special boundary that are normally referred to as absorbing, silent, anechoic, nonreflecting or transmitting boundaries, or, alternatively, as infinite elements. The purpose of these special boundaries or elements is to prevent wave reflections at the edges of the mathematical models used, which, by necessity, must remain finite in size. A number of these boundaries have been proposed in the past with recourse to various mathematical or physical principles. It was proven in [3] that all of them are mathematically equivalent, and therefore they must have comparable wave-absorbing attributes. Unfortunately, none of the transmitting boundaries can fully prevent all possible reflections under the full range of possible incident angles.

Some of the difficulties named above could be overcome by implementation of the moving window method. In the moving window method the load is kept still, and the finite element model of the railway track moves in the direction opposing the originally assumed load movement. This can be achieved by several ways. Either the finite elements are altered in order to implement the effect of the load velocity [4], or results are shifted against the load. Sometimes it is possible to pull only a part of the model at a steady speed, for instance an imaginary strip containing the wheel/rail irregularities. This procedure is called the moving irregularity model [5]. In [6] a beam on elastic foundation subjected to a moving force was

considered. The deflection and velocity profile of the current time step were translating back and used as initial conditions for the next time step. Procedure was implemented in the Newmark method. The moving window method is also implemented in [7]. In [6, 7] the rail is modeled as simply supported beam and no care is taken about reflected waves, the beam lengths are 30m and 62.4m, respectively, which cannot be considered as a very long beam.

A shift of results is not simple to accomplish in commercial finite element software, because such an operation is usually protected against inappropriate using the software. Therefore other considerations must be taken into account. One of the new contributions of this paper is the establishment and implementation of the Enhanced Moving Window Method (EMWM) in commercial finite element software. The method is tested on one-, two- and three-dimensional models. It is shown that the quasi-stationary response of an infinite structure can be obtained with sufficient accuracy, which significantly reduces the calculation time by reduction of both the model size and the necessary analysis time. The quasi-stationary (quasi steady-state) response of an infinite structure subjected to one single load can be numerically obtained by the so-called long simulation on a large model (LSLM). In the first part of the EMWM the window is formed around the load and the boundary conditions used on the front and rear faces of the window in fact reflect the situation where equally spaced loads travel on an infinite structure. These loads are distributed in the way that each load stays within one window and the quasi-stationary response beyond it is negligible. It will be shown that such a result corresponds to a satisfactory approximation of the quasi-stationary response induced by a single load on an infinite structure. After that other boundary conditions can be implemented by means of one recovering step.

The EMWM can be simply generalized to account for periodically distributed inhomogeneities in the longitudinal direction. The EMWM is also valid in the geometrically nonlinear range and reversible physically nonlinearity range if the same loading and unloading paths are followed. In the linear case the effect of a set of loads can be obtained by superposition. However, in order to implement (i) a set of loads in the nonlinear case and (ii) an irreversible physical nonlinearity (*e.g.* plasticity), further consideration must be taken. As another new contribution of this paper, it is suggested to solve these issues by time-dependent boundary conditions (T-DB). At first, quasi-stationary results are obtained for reversible nonlinearities. Then these results are used to provide the time dependent boundary conditions on front and rear faces of the model. Loads are placed on the finite element track model and let travel until they reach the front face. Subsequent loads are placed on the model with accumulated plastic deformations. When the distance of the subsequent loads is too small, they must be placed at the same time. In this case the time dependent boundary conditions should be obtained by superposition of the previous results. When the distance between loads is large enough, the model is let free of loads until the next load is placed.

The EMWM solves the problem of the boundary conditions on the front and rear faces of the model. Regarding the bottom face, other considerations must be taken. In reality the soil, when subjected to a certain loading history, has the ability to memorize the highest level of loading, which can be mathematically represented by the over-consolidation ratio and initial

void ratio. In its virgin state, the soil deformability is relatively high. But following the unloading/reloading path shows almost negligible deformation until the highest stress the soil has experienced ever before is reached again [8]. The so-called active depth (zone), which stands for the depth of the deformable soil, is not very high and can be determined experimentally. In this contribution the active depth is assumed to have a certain value. Then a method is proposed to define the boundary conditions on the bottom surface allowing reducing the model depth.

The EMWM has the following limitations: (i) only subcritical velocities can be considered, because the significant deflection field must be limited; (ii) at least light damping must be added. Implementation of supercritical velocities could only be possible under very high damping in order to keep the significant deflection field limited within a reasonable model size, otherwise, the main gain, which is the computational time reduction, is lost. Some of the advantages are listed as: (i) the model itself can be rather small, but the time dependent results extracted can cover an arbitrarily large model; (ii) nonlinearities can be introduced; (iii) calculation time is acceptable; (iv) transmitting boundaries on the front and rear faces of the model do not have to be implemented in the first part.

The EMWM and its extension by the T-DB is implemented in the ANSYS software [9]. Numerical procedures are automated using the ANSYS Parametric Design Language. Accuracy is verified by comparison with analytical solutions and long simulations on large models. The L^2-norm is used for accuracy evaluation. The paper is organized in the following way: in Section 2, one-dimensional case studies are analyzed. In Section 3, two-dimensional cases are presented, either with or without the periodic inhomogeneities. Further, in Section 4, extensions by the T-BD are described and irreversible nonlinearities are implemented. In Section 5, three-dimensional case studies are given and the paper is concluded in Section 6.

2. ONE-DIMENSIONAL CASE STUDY

2.1. The improved window method

Let an infinite beam on a visco-elastic foundation traversed from left to right by a uniformly moving load be assumed. Such a problem has an analytical solution in form of a quasi-stationary response, which is well-documented in several works, *e.g.* in the monograph [10]. Numerically these results can be obtained by the so-called LSLM. This means that the load should be firstly imposed quasi-statically at a reasonable distance from the rear extremity of a long beam, and then let to travel in the direction to the front extremity until its deflection, velocity and acceleration profiles stabilize. Such a procedure is time consuming. Especially for velocities close to the critical one there is a significant part of the transient response which must be numerically attenuated.

The moving window method creates a window of reduced dimensions around the load and moves the model instead of the load. Generally, this method should allow studying non-homogeneous effects and other influences. However, commercial software is usually

protected against results movement to other positions where these results are used as the previous time step response and thus should be used in the next time step.

There is the possibility to extract the displacement and velocity fields, shift them in the sense opposite to the assumed load movement and use them as initial conditions. Such a procedure is numerically sensitive. First of all, if results are shifted in a standard way, any kind of boundary conditions will not be satisfied by the initial fields, as it is shown in Figure 1.

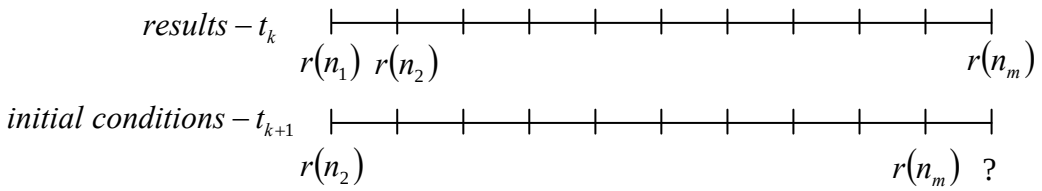

Figure 1. Standard results shifting – issue 1.

For instance, let n_1 be the rear boundary node and n_m the front boundary node (*m* stands for the total number of nodes). If results obtained in the time step t_k will be shifted, then the result $r(n_1)$ in n_1 will not be used but the result $r(n_2)$ which was obtained in the interior node n_2 will be placed in the rear position without fulfilling the boundary conditions. On the other hand $r(n_m)$ will be placed in an interior node and a result to be applied on the boundary node n_m is missing. Another issue is that the initial conditions in form of displacement and velocity fields do not recreate the acceleration field correctly, because the relative position of the load is different, as it is demonstrated in Figure 2.

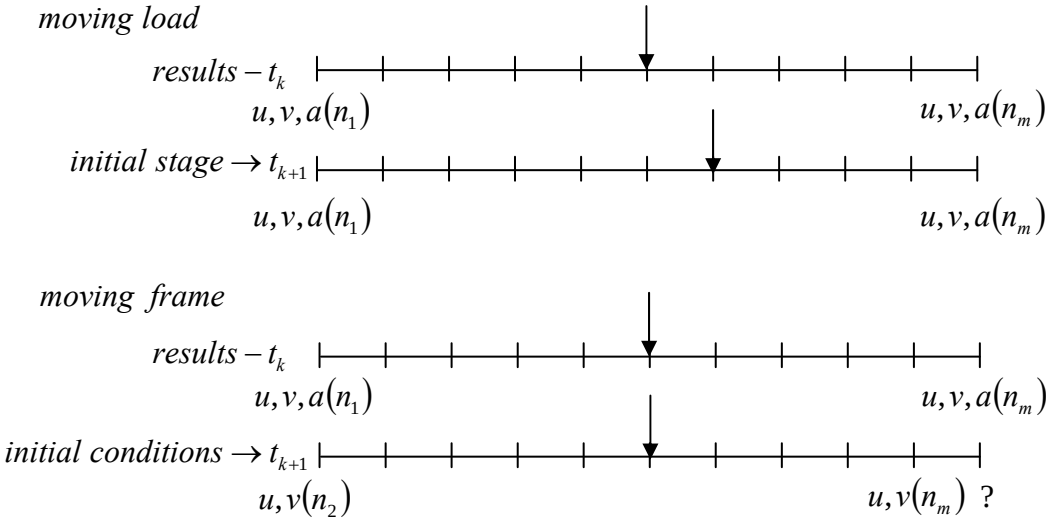

Figure 2. Standard results shifting – issue 2.

These facts seem to be of low importance. The discrepancies are not noticeable in first time steps, but along the time interval the small numerical errors accumulate until the solution loses its numerical stability. Several possibilities of shifting schemes and boundary conditions were tested. It was concluded that the best numerical performance is achieved when: (i) the model window is selected in the way that the response field beyond the window is negligible; (ii) for quasi-stationary solution the periodic boundary conditions are imposed; (ii) the time steps are separated in two parts: in the first part the results just obtained are used as initial conditions that are shifted back together with the load and a conveniently small time step $\delta\Delta t$ is applied in order to reaplicate the acceleration field; in the second part the load moves forward, and the step is completed to Δt as it is explained in Figure 3. We will name the method as Enhanced Moving Window Method (EMWM).

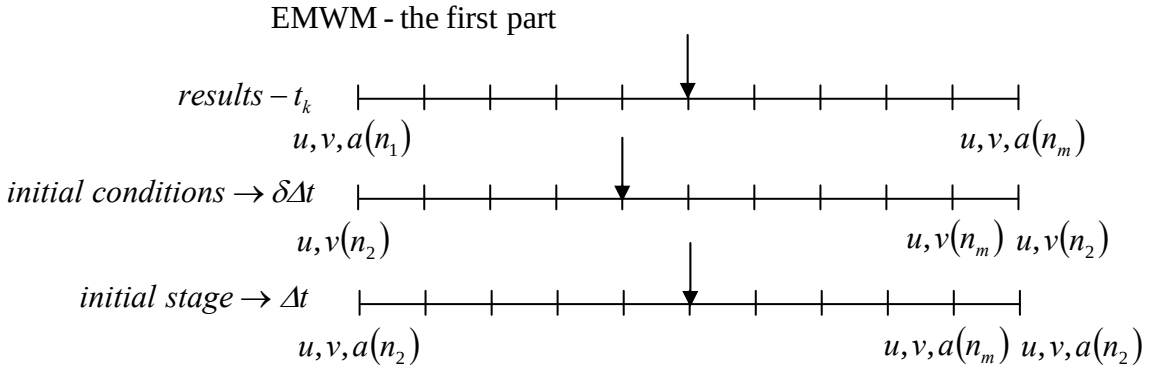

Figure 3. The first part of the EMWM.

The EMWM is numerically stable. Nevertheless, in order to obtain pretended results with acceptable error and efficiently, three issues must be carefully considered: (i) the size of the window; (ii) the size of the elements; (iii) the level of damping. If the window size is too large, the computation will be unnecessarily long, while if it is too small then the stabilized results will not correspond to the infinite model. The element size will naturally help to improve accuracy; the damping will speed up the convergence. If no damping is assumed, then the transient part of the response will not attenuate. No numerical instability occurs, the deflection field will oscillate around the quasi-stationary solution and a very low decreasing tendency in L^2-norm of the difference field is observed. It is worthwhile to mention that for the beam structure, besides deflection and velocity fields, rotation and rotational velocity fields must also be considered.

In the case study of this section the beam is modeled as two UIC rails and the load corresponds to a common value of the axle load, P=200kN. Numerical input data are summarized in Table 1. A very soft foundation is chosen in order to visualize better the deflection field. The method is tested with respect to the beam length, the element size, the load velocity and the level of damping. The accuracy is evaluated by L^2-norm of the difference field, determined as subtraction of the analytical and numerical solutions.

Implementation of a realistic damping behavior is not a simple task. It is impossible to introduce geometrical damping in such a simplified model. Material damping should encompass both the internal friction in the beam (usually assumed as viscous damping and defined by the damping ratio) as well as the damping of the geomaterial representing the foundation. The material damping of the foundation is commonly expressed by a damping coefficient c of distributed dashpots, which is a value independent of frequency. In fact, this coefficient should be attributed to the hysteretic damping, which is more adequate for geomaterials.

Property	Beam (2 UIC60)
Young's modulus E (GPa)	210
Poisson's ratio	0.3
Density ρ (kg/m^3)	7800
Transversal section area A (m^2)	$153.68 \cdot 10^{-4}$
Moment of inertia I (m^4)	$6110 \cdot 10^{-8}$
Bending stiffness EI (MNm^2)	12.831
Foundation stiffness k (MN/m^2)	1
Mass per unit length μ (kg/m)	119.8704

Table 1. Characteristics of 2UIC60 rails.

In this paper the damping is defined by the equivalent distributed damping coefficient assuring the same level of damping in lightly damped scenarios, derived and justified in [11]

$$c = 2\xi\sqrt{2k\mu}\,. \tag{1}$$

Relation (1) means that practically same results are obtained if either damping in rails is defined by the damping ratio ξ (and no damping is attributed to the foundation) or the damping coefficient c is given by (1) and no damping in rails is assumed, or any combination of these values. It is necessary to point out that the critical damping of the infinite beam on elastic foundation is defined differently and depends on the load velocity, [10]

$$c_{cr} = \frac{2}{q}\sqrt{\frac{2}{27}k\mu\left(-q^2+\sqrt{q^4+3}\right)}\left(2q^2+\sqrt{q^4+3}\right) \tag{2}$$

where

$$q = \frac{v}{v_{cr}} = v\sqrt[4]{\frac{\mu^2}{4kEI}} \tag{3}$$

In ANSYS software the damping specified in the case studies was introduced as the mass damping.

2.2. Results stabilization and convergence

At first, the results stabilization and convergence is tested with respect to the beam length. Beam lengths of 200m, 60m and 36m are considered.

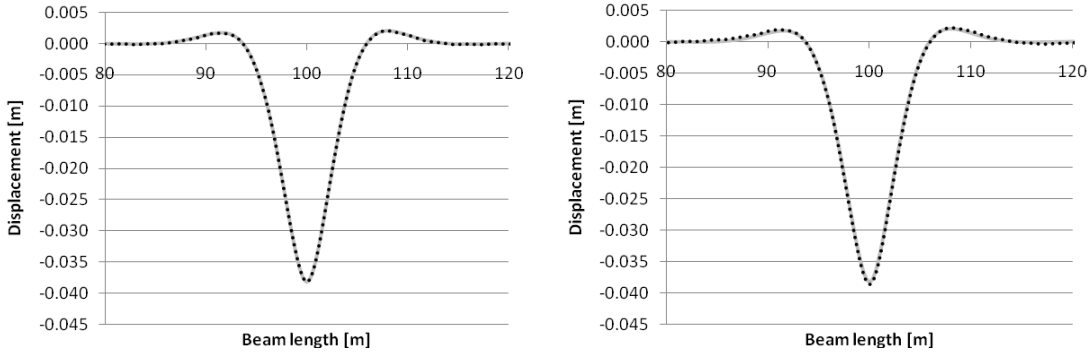

Figure 4. Results comparison on a reduced length: the analytical solution (grey solid line) versus the EMWM solution (black dotted line), 500th and 30th time step on the left and right figures are shown, respectively.

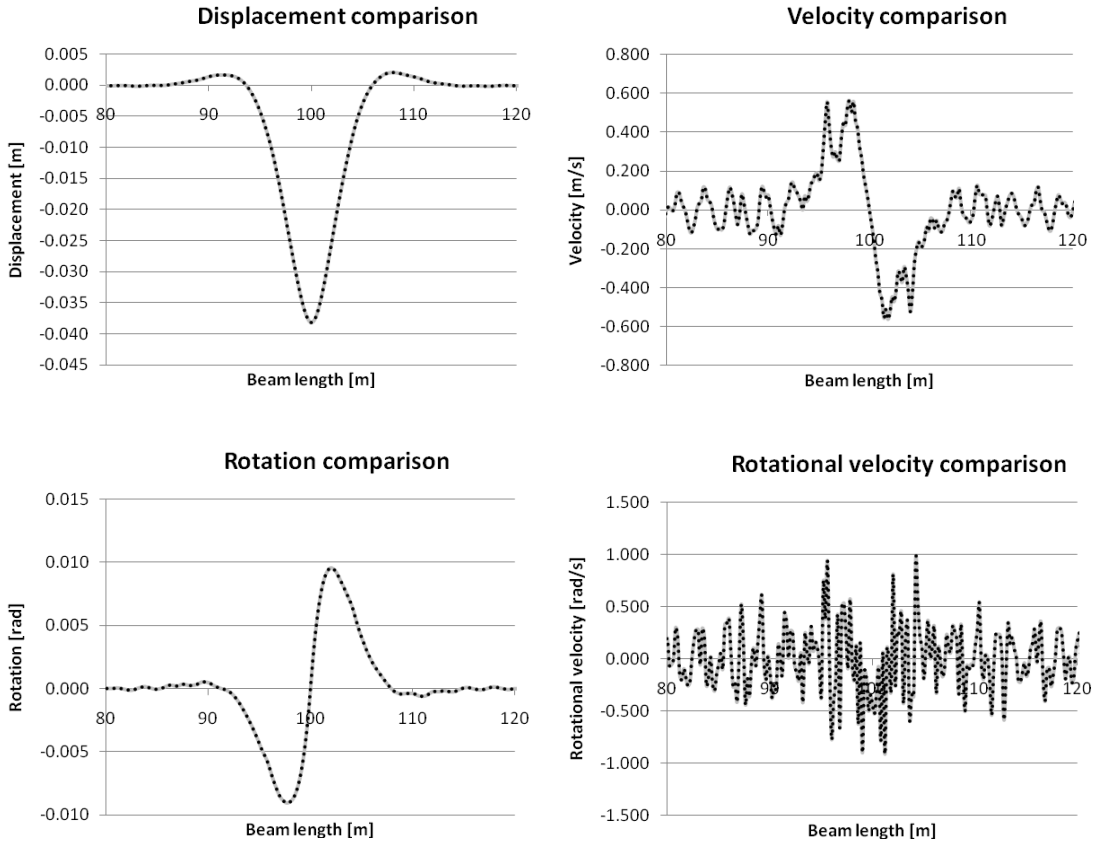

Figure 5. EMWM results on a reduced length, 200th (grey solid line) and 500th time step (black dotted line).

The other numerical input data are: the element size d_e=0.2m, the load velocity v=50m/s and the damping ratio ξ=0.1. This means that the equivalent damping coefficient of the foundation is c=3097Ns/m^2, which can be introduced in ANSYS software as mass coefficient α=25.83s^{-1}. In this case the critical velocity is v_{cr}=244.47m/s, thus q=0.205 and c_{cr}=67229.2Ns/m^2. Therefore this level of damping represents 4.6% of the critical damping. In Figure 4 the EMWM results on a reduced length of 200m-long beam are shown. It is seen that the results coincidence is excellent and that it was satisfactory after the 30th time step. In Figure 5 it is verified that there is no lack of numerical stability in the EMWM. Full results comparison is done after 200 and 500 time steps. The 500th time step represents in this case 100m load travelled distance. In Figure 6 the deflection field obtained for the beam lengths L=36m and 200m are compared.

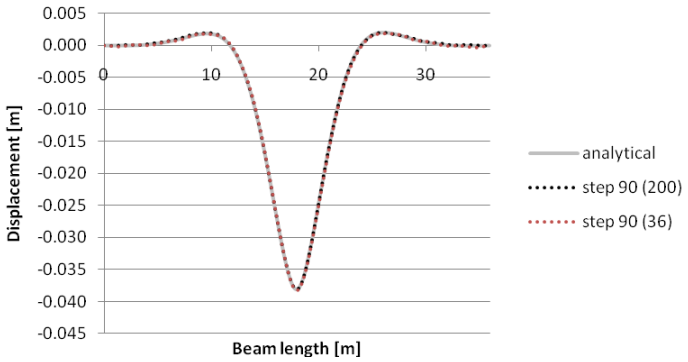

Figure 6. Results comparison. Numerical results correspond to 90th time step, the number in parentheses stands for the beam length.

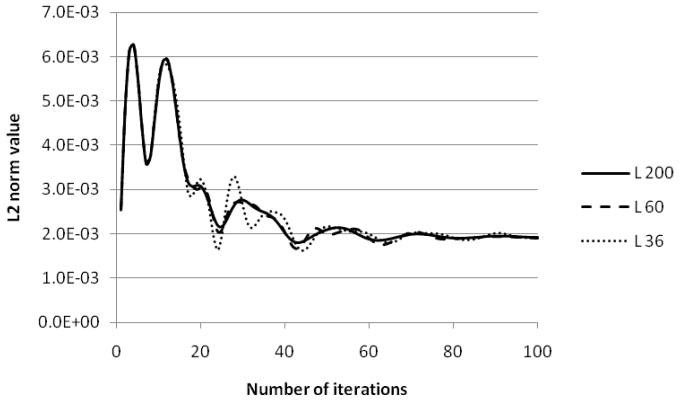

Figure 7. Convergence rate represented by L^2-norm of the difference field, comparison of different beam lengths.

The convergence rate is evaluated by plotting the L^2-norm of the difference field. In Figure 7 it is seen that the beam length does not contribute to the convergence rate. In the legend the number of iterations means the same as the number of time steps. One might remark that the

integral is taken over very different domains, nevertheless, the extension from L=36m to L=60m and L=200m is by insignificant displacement values, therefore the comparison is meaningful. It is seen, however, that the error tends to a fixed value, impossible to remove. The final error is attributed to small oscillations around the analytical deflection, which stay at the same positions, and are formed around insignificant values. These inaccuracies could be improved by reducing the element size. In Figure 8 a detail of the deflection field is shown on the 36m-long beam with element sizes d_e=0.2m and 0.1m, respectively.

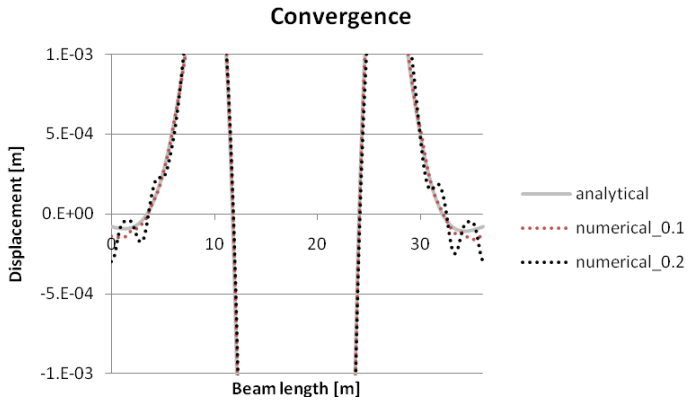

Figure 8. Detail of the displacement field: improvements attributed to the element size.

2.3. Velocity and damping influence

At first, the EMWM is tested with respect to the load velocity. In Figure 9 it is seen that analytical and numerical results match for v=100m/s, 150m/s and 200m/s on beam lengths L=24m, 30m and 36m, respectively (d_e=0.2m).

In addition, it is shown that the rate of the convergence can be highly improved by the damping increase. It is known that the presence of damping distorts the quasi-stationary deflection to a non-symmetrical shape. A highly damped case (ξ=1, which means 46% of the critical damping) is tested in order to confirm better the coincidence with the analytical solution. In Figure 10 results are presented for L=24m, v=50m/s and d_e=0.2m.

Further, the damping influence on the convergence rate is tested. Results are presented in Figure 11 for v=50m/s, L=36m, d_e=0.1m and ξ=0, 0.1 and 0.05, respectively. It is confirmed that the case without damping has very low convergence rate. In Figure 12 it is shown extension to 20000 iterations (time steps).

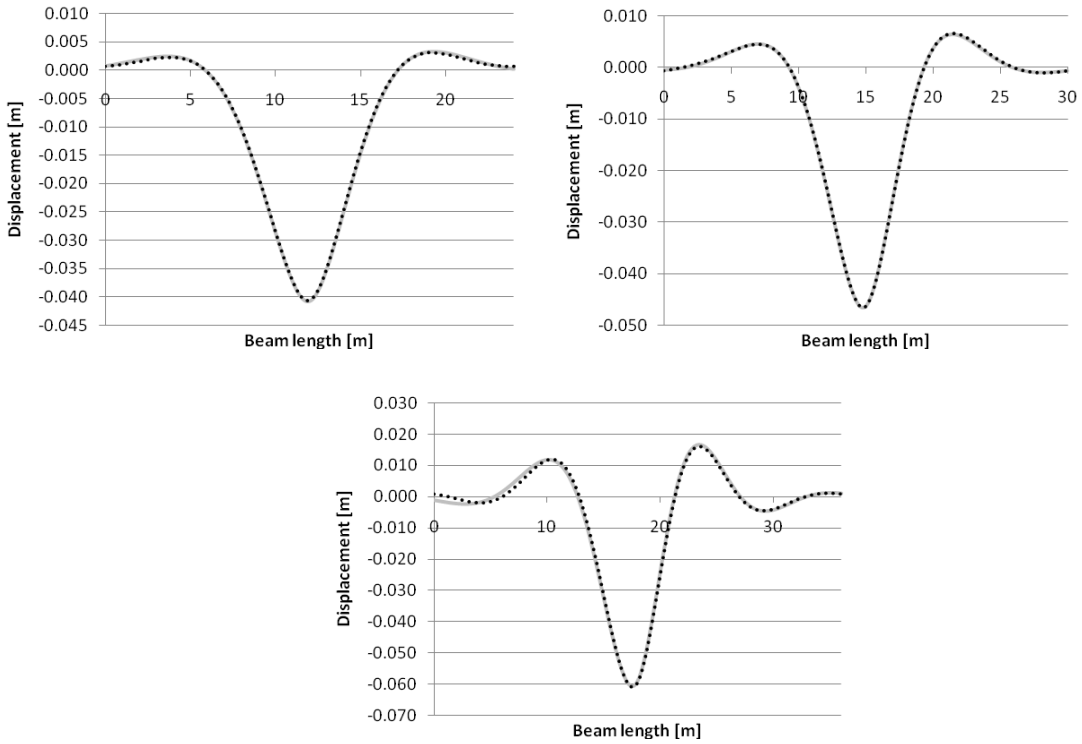

Figure 9. EMWM results convergence: v=100m/s (top left), 150m/s (top right) and 200m/s (bottom); analytical (grey solid line) versus numerical results (black dotted line).

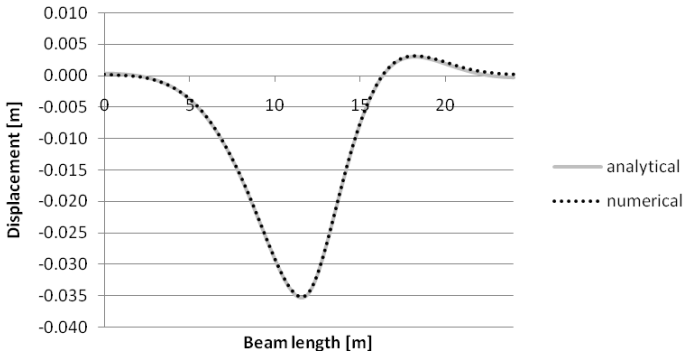

Figure 10. Results convergence in highly damped case.

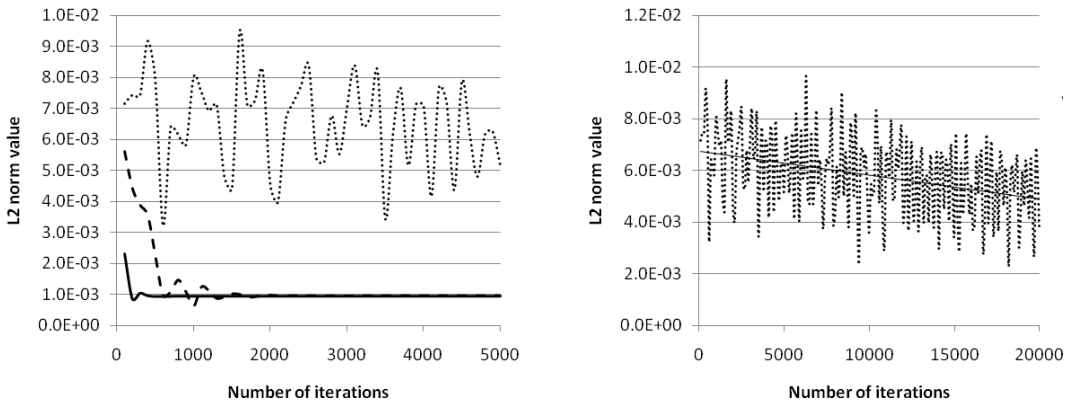

Figure 11. Convergence rate represented by the L^2-norm of the difference field: comparison of different damping values: ξ=0 (black dotted line), ξ=0.1 (black dashed line), ξ=0.05 (black solid line). On the right extension to 20000 iterations of the undamped case is shown together with the linear trend line.

2.4. Set of loads and time dependent boundary conditions

It is useful to present the extension of the EMWM allowing accounting for more loads. When the forces are relatively close to each other, they can be placed on the structure at the same time. Alternately, in the linear case, results can be superposed. The results in Figure 12 correspond to deflection field induced by two equal forces P=200kN distanced by 3m. The effect of successive loads can be studied more efficiently by introduction of the T-DB. This means that once the quasi-stationary results are obtained, they can be used in form of boundary conditions, while the load is moving on the structure. For consecutive loads the corresponding boundary conditions are obtained by superposition.

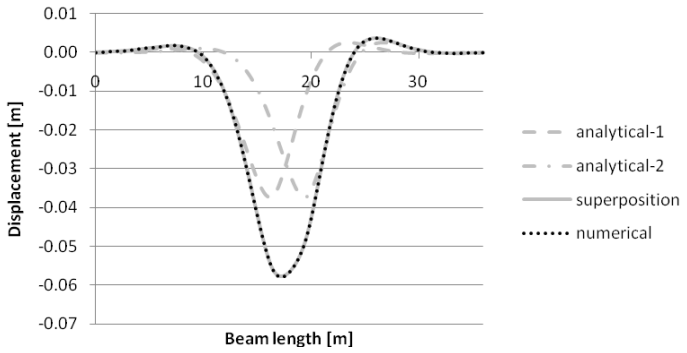

Figure 12. Effect of two forces: comparison with superposition of the analytical results.

The implementation of the T-DB can be made by two approaches. In the first approach the load is placed in the middle of the structure and moved to the right, while the rear beam extremity is fixed and the front beam node movement is directed by the results obtained previously. In the second approach the structure is reduced by half, the load is placed in the rear node and moved to the front node, while both beam extremities are directed by the T-DB.

Small differences in results are detected because only displacements and rotations can be imposed in the rear and front nodes of the structure. Results are summarized in Figures 13 and 14. In these figures the deflection fields obtained are shifted back for visualization and comparison with the quasi-stationary shape.

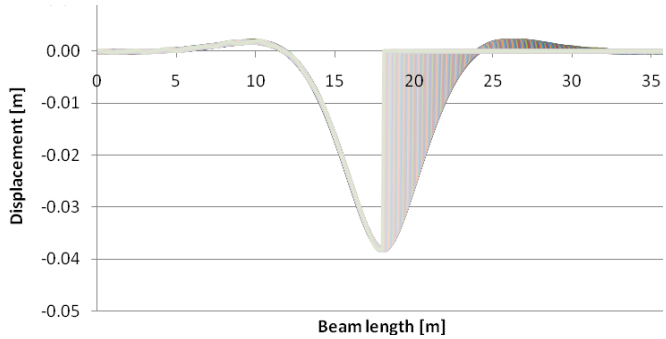

Figure 13. The T-DB: first approach.

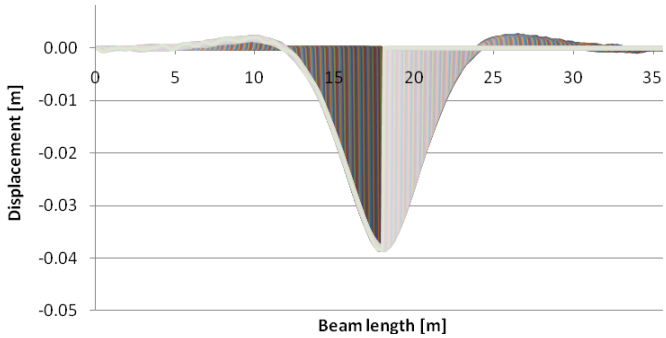

Figure 14. The T-DB: second approach.

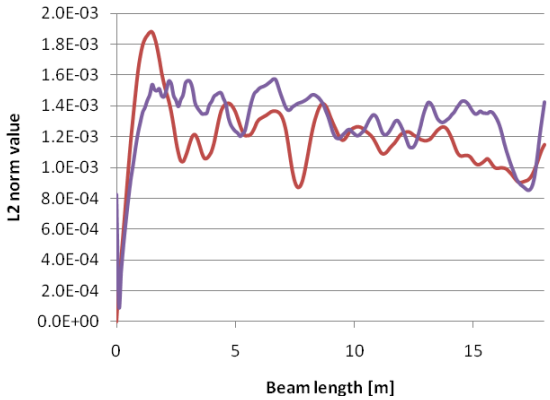

Figure 15. The T-DB approaches comparison by the L^2-norm of the difference field (red solid line – first approach, violet solid line – second approach).

The error is analyzed by the L^2-norm in Figure 15. It can be concluded that the performance of both approaches is practically the same.

3. TWO-DIMENSIONAL CASE STUDY

In the two-dimensional case studies two models are considered. In the first one a beam is placed on a soil and in the second one, besides these components, sleepers and ballast layer are also modeled. The beam corresponds to two UIC60 rails and the soil is characterized by pressure and shear waves velocities of propagation v_p=187m/s, v_s=100m/s and density of 1850kg/m^3. The properties of other components are summarized in Table 2.

Property	Sleeper	Ballast
Young's modulus E (GPa)	30	0.2
Poisson's ratio	0.2	0.1
Density ρ (kg/m^3)	2054	1850
Depth (m)	0.2	0.6
Length (m)	0.2	---

Table 2. Characteristics of sleepers and ballast.

The EMWM is firstly verified on the first model. Then, on the second model the EMWM extension to periodic inhomogeneities in the longitudinal direction is validated. For the sake of simplicity sleeper dimension is matched to the element size d_e=0.2m. Their distance is kept as 0.6m. The plane elements in the ANSYS model are assumed under plane strain conditions.

3.1. Model depth

In the two-dimensional case study it is important to set correctly the model depth and the boundary conditions on the bottom line. It is incorrect to approximate the soil layer by the semi-infinite elastic plane. Deep soil layers are usually much stiffer and, moreover, the soil memorizes the highest level of loading and shows almost negligible deformation until the highest stress the soil has experienced ever before is reached [8]. The so-called active depth (zone), which stands for the depth of the deformable soil, should be determined experimentally. At such a level the boundary displacements can be fixed.

It is proposed a reduction of the model depth by representative springs and viscous boundary according to [12]. The representative distributed elastic springs are defined as:

$$k_n = \frac{\lambda + 2\mu}{H - h} = \frac{E(1-\nu)}{(1+\nu)(1-2\nu)(H-h)}, \tag{4}$$

$$k_t = \frac{\mu}{H - h} = \frac{E}{2(1+\nu)(H-h)}, \tag{5}$$

where k_n and k_t stand for the spring rigidities in normal and tangential directions, respectively, and λ, μ, E, ν are elastic constants: two Lame´s constants, Young´s modulus

and Poisson´s ratio of the omitted soil. H represents the active depth and h the depth of the soil in the model. For non-homogeneous active depth the spring constants must be composed.

First of all, results independence on the model depth is analyzed. The active depth is chosen as H=12m and the model depth h is varied between 10m, 8m, 6m and 4m. No analytical results are available, therefore the EMWM results are compared with the LSLM results in Figures 16, 17 and 18. Very good results coincidence is obtained until h=6m. In Figure 16 the beam stabilized deflection is shown. All deflections shown in this figure should be coincident, because the results should not depend on the model depth for a fixed active depth. It is seen, however, that for the shallow model (h=4m) the discrepancies are already too large. It was verified by the LSLM that they are attributed to the representative springs definition and not to the EMWM. In Figures 17 and 18 the vertical and horizontal displacements in the vertical soil cut under the load are plotted. It is seen that coincidence in vertical displacements under the load is excellent, while discrepancies can be found in horizontal displacements. The horizontal displacements are one order less than the vertical ones, therefore the absolute error is not very significant.

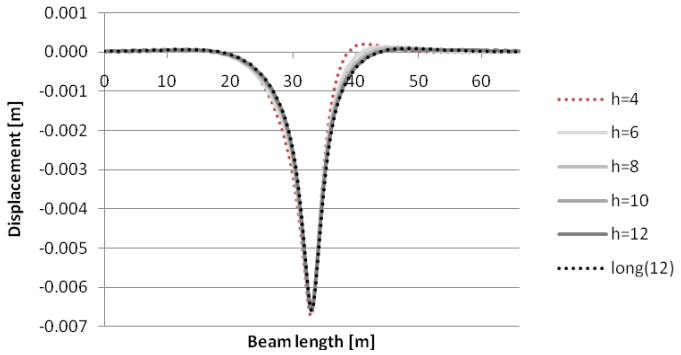

Figure 16. Beam vertical deflection: black dotted line stays for the LSLM; h in the legend represents the model depth, red dotted line marks the results which are deviated from the correct ones.

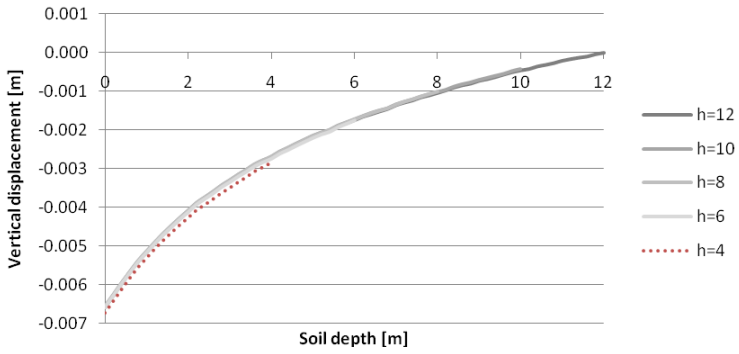

Figure 17. Soil vertical deflection under the load: black dotted line stays for the large model; h in the legend represents the model depth, red dotted line marks the results which are deviated from the correct ones.

Nevertheless, it can be concluded that the definition of the horizontal springs should be

improved. In all presented cases the damping is defined by ξ=0.1 and a representative spring of the full soil layer calculated according to equation (4) with h=0. These two values define c by equation (1), which yields the mass coefficient α=15.28s^{-1} to be introduced in the ANSYS software.

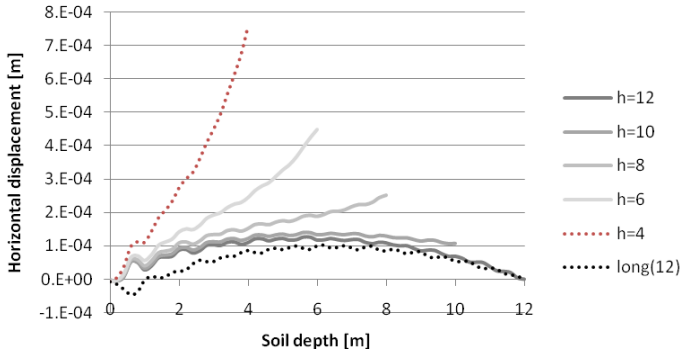

Figure 18. Soil horizontal deflection under the load: black dotted line stays for the large model; h in the legend represents the model depth, red dotted line marks the results which are deviated from the correct ones.

The effect of different velocities is analyzed on the shallow model of h=4m. Results are plotted in Figure 19.

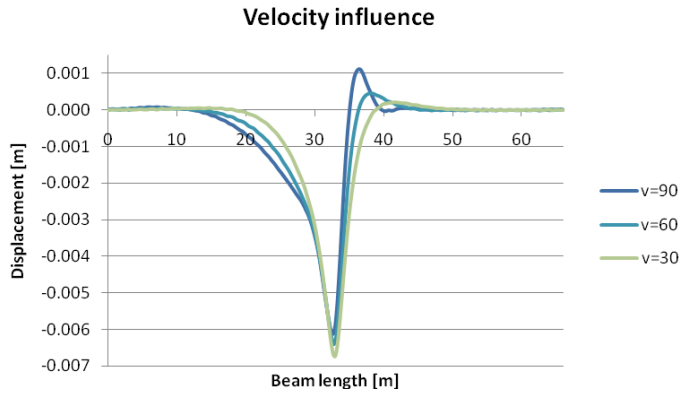

Figure 19. Beam vertical deflection: velocity influence on the shallow model (values in the legend are in m/s).

Further, the second model is tested. The geometry detail of the shallow model (h=4m) is shown in Figure 20. Depending on the required precision, calculations take 10-30 minutes.

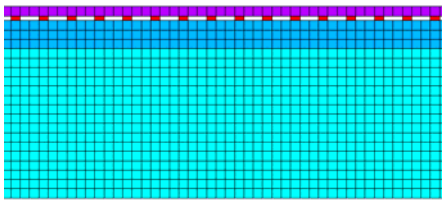

Figure 20. The geometry detail of the second model: the shallow version with h=4m.

The extension to periodic non-homogeneities is tested by results independency on the starting load position. Perfect results coincidence is obtained. Displacement fields are shown in the full model in Figures 21 and 22.

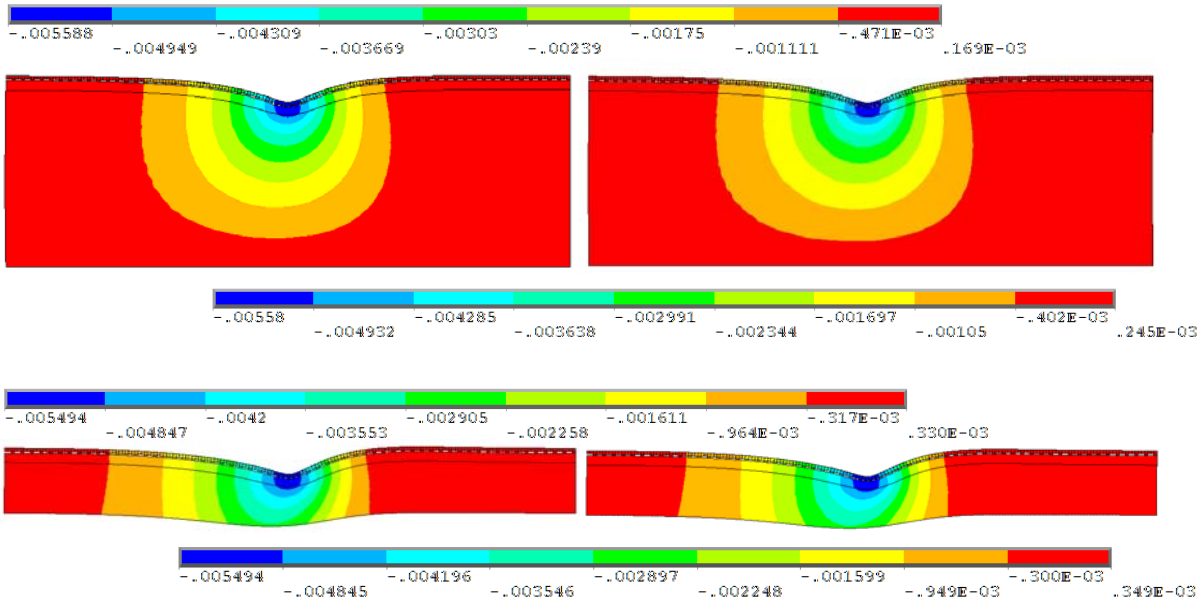

Figure 21. Vertical displacement field of the full (H=h=12m)and the shallow model (h=4m): the detail of the LSLM results (left) and the EMWM results (right). Values are in [m], the legend of the LSLM is on the top of figures and of the EMWM on the bottom of the figures.

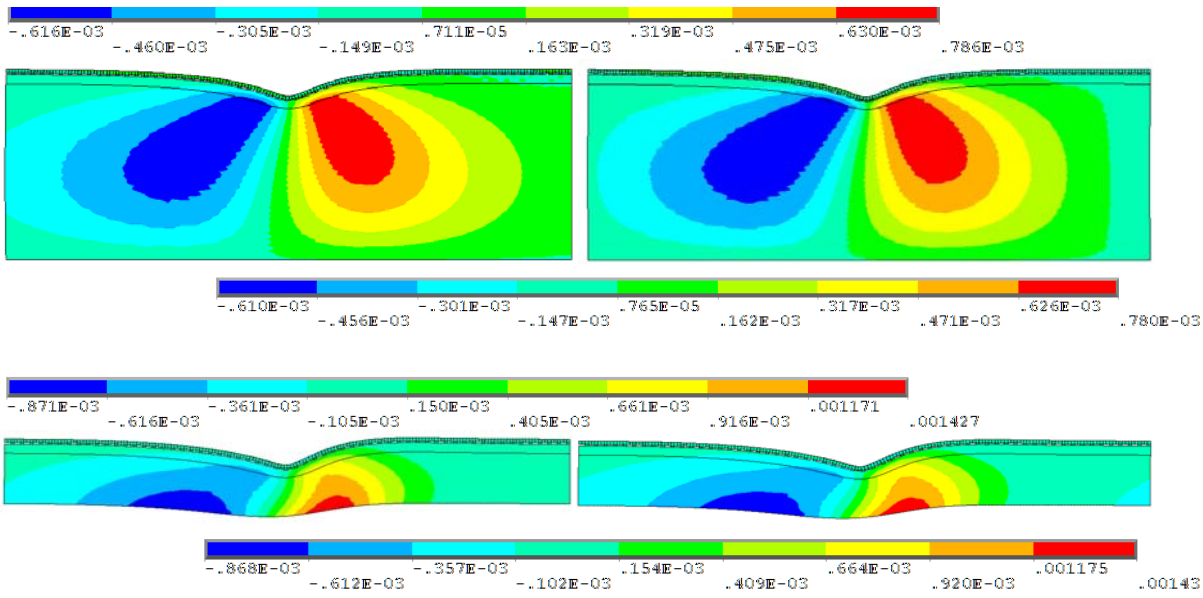

Figure 22. Horizontal displacement field of the full (H=h=12m)and the shallow model (h=4m): the detail of the LSLM results (left) and the EMWM results (right). Values are in [m], the legend of the LSLM is on the top of figures and of the EMWM on the bottom of the figures.

Detail of the LSLM and EMWM results on the same model length of 36m are compared for h=12m and h=4m. Similarly as in the previous case, it is confirmed that the discrepancies in the shallow model are attributed to the representative horizontal spring definition and not to the EMWM.

4. TIME-DEPENDENT BOUNDARY AND PLASTICITY

In this section the extension of the EMWM by the T-DB is presented in order to account for irreversible nonlinearities. For the sake of simplicity a test case with no connection to railway applications is chosen for the preliminary analysis. The first model from Section 3 is selected with the active depth and the model depth as H=h=4m and the model length as L=36m.

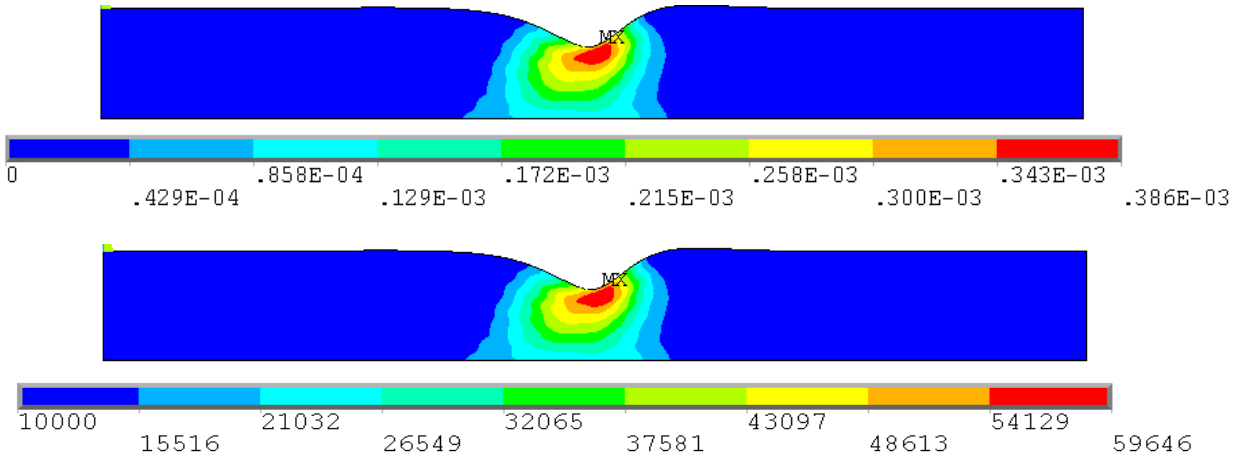

Figure 23. Equivalent plastic strain (above) and stress (bellow, in Pa) obtained by the application of the EMWM.

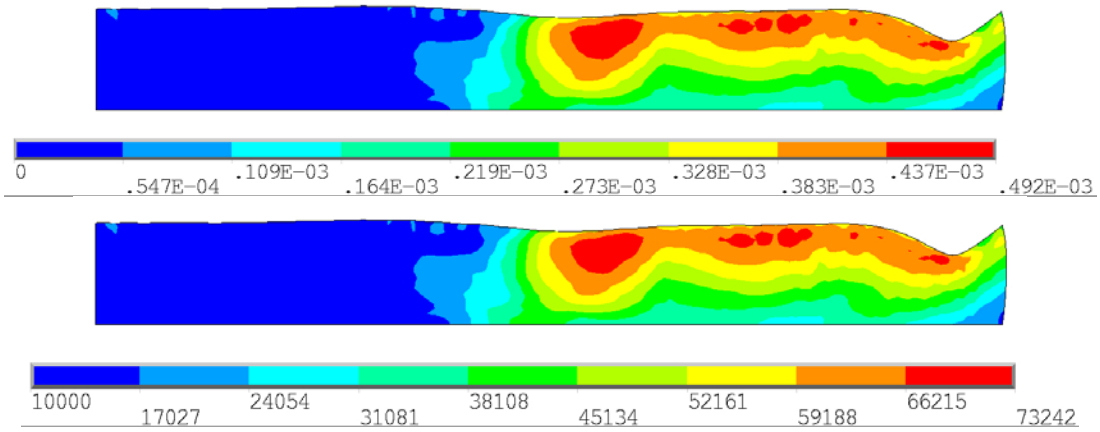

Figure 24. Equivalent plastic strain (above) and stress (bellow, in Pa) obtained by the application of the extended EMWM by the first approach of T-DB.

The bilinear von Mises plasticity with isotropic hardening is added to the soil behavior. The

yield stress is introduced as 10kPa and the tangent modulus of elasticity as 35MPa. Firstly, it is confirmed that by simple implementation of the EMWM the plastified regions are only concentrated below the load, which means that the regions plastified previously completely recovered, which does not correspond to the reality (Figure 23). In Figure 24 results obtained by the extension of the EMWM by the first approach of the T-DB are presented. Results presented must be confirmed by the LSLM. Introduction of realistic ballast failure behavior is the subject for the further research.

5. THREE-DIMENSIONAL CASE STUDY

The three-dimensional case study models the real railway track documented in [13]. For the preliminary results the model is simplified by symmetry and only one substrate layer of h=2m is implemented. It is further assumed that the active depth is equal to this depth, i.e. that H=2m. The rail pads influence is omitted and thus a rigid connection between the rail and sleeper is introduced. A three-dimensional model has one more boundary which has not been discussed in this paper yet. It is the lateral boundary. This boundary is modeled as the viscous boundary according to [12].

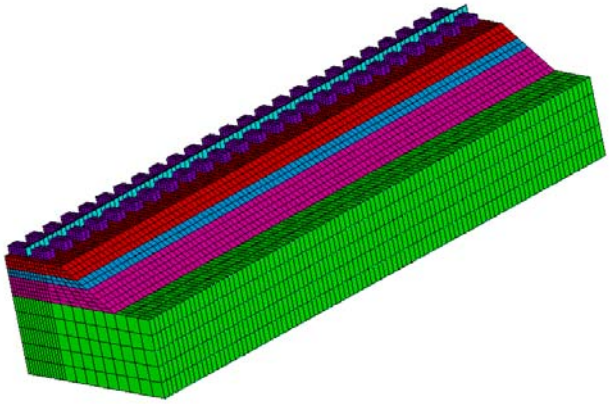

Figure 25. The three-dimensional model of 15m length.

In Figure 25 the geometry of the model is shown. The stabilized results obtained by the EMWM after 15 iterations are compared with the results obtained on a longer model of 30m by the LSLM. Some differences are detected, especially for lower velocities, but it is necessary to point out, that the 30m-long model is not large enough to be representative. In the large model the viscous boundary is also applied on the front and rear faces.

6. CONCLUSIONS

In this paper two new approaches are presented. They are designated as the EMWM and extension o this method by the T-DB. Both methods are numerically stable. These methods have as its objectives: (i) determine the quasi-stationary response to a moving load; (ii) account for consecutive loads and accumulated irreversible nonlinearities. Cases studies presented demonstrate that the objectives are fulfilled.

REFERENCES

[1] Z. Dimitrovová and J.N. Varandas, "Critical velocity of a load moving on a beam with a sudden change of foundation stiffness: applications to high-speed trains", *Computers & Structures*. Vol. **87**, pp. 1224–1232, (2009).

[2] Z. Dimitrovová, "A general procedure for the dynamic analysis of finite and infinite beams on piece-wise homogeneous foundation under moving loads", *Journal of Sound and Vibration*. Vol. **329**, pp. 2635–2653, (2010).

[3] E. Kausel, "Local transmitting boundaries", *Journal of Engineering Mechanics.* Vol. **114**, pp. 1011-1027, (1988).

[4] A.W.M. Kok, "Finite element models for the steady state analysis of moving loads", *Heron*. Vol. **45**, pp. 53-61, (2000).

[5] K. Knothe and S.L. Grassie, "Modelling of railway track and vehicle/track interaction at high frequencies", Vehicle System Dynamics. Vol. **22**, pp. 209–262, (1993).

[6] J-S. Chen, Y-K. Chen, "Steady state and stability of a beam on a damped tensionless foundation under a moving load", *International Journal of Non-Linear Mechanics*. Vol. 46, pp. 180-185, (2011).

[7] L. Wu, Z.F. Wen, X.B. Xiao, W. Li and X.S. Jin, *Modeling and analysis of vehicle-track dynamic behavior at the connection between floating slab and non-floating slab track*, B.H.V. Topping, J.M. Adam, F.J. Pallarés, R. Bru e M.L. Romero (editors), Civil-Comp Press, Stirlingshire, UK. *10th International Conference on Computational Structures Technology* (CST2010), Valencia, Spain (2010), p. 20.

[8] J.E. Bowles, *Foundation analysis and design*, McGraw Hill, (1968).

[9] ANSYS, Inc. Documentation for Release 12.1, Swanson Analysis Systems IP, Inc., November 2009.

[10] L. Frýba, *Vibration of solids and structures under moving loads*, Research Institute of Transport, Prague (1972), 3rd edition, Thomas Telford, London, (1999).

[11] Z. Dimitrovová, A.F.S. Rodrigues, *Critical velocity obtained by simplified models of the railway track: viability and applicability*, B.H.V. Topping, J.M. Adam, F.J. Pallarés, R. Bru e M.L. Romero (editors), Civil-Comp Press, Stirlingshire, UK. *10th International Conference on Computational Structures Technology* (CST2010), Valencia, Spain (2010), p. 36.

[12] J. Lysmer, R.L. Kuhlemeyer, "Finite dynamic model for infinite media", *Journal of the Engineering Mechanics Division, ASCE*, Vol. **95(EM4)**, pp. 859-877, (1969).

[13] "Definição de caso de estudo de um trecho de via-férrea para simulação numérica", Internal report on POCI/ECM/61114/2004 grant, Minho University, 2006 (in Portuguese)